Catal Lett (2009) 129:7–11
DOI 10.1007/s10562-009-9856-7

Preferential Oxidation of CO Impurities in the Presence of H_2 on NiO-Loaded and Unloaded TiO_2 Photocatalysts at 293 K

Takashi Kamegawa · Tae-Ho Kim · Jun Morishima · Masaya Matsuoka · Masakazu Anpo

Received: 17 July 2008 / Accepted: 5 January 2009 / Published online: 23 January 2008

Abstract The photocatalytic preferential oxidation of CO with O_2 in the presence of H_2 (photo-PROX) was found to proceed efficiently on the NiO-loaded TiO_2 (NiO/TiO_2) catalyst under UV light irradiation at 293 K. NiO/TiO_2 exhibited higher CO conversion as well as CO_2 selectivity for a photo-PROX reaction than the original unloaded TiO_2 (P-25). Various spectroscopic investigations have revealed that the small NiO clusters formed on TiO_2 play an important role in the enhancement of CO oxidation activity in this reaction.

Keywords NiO/TiO_2 · TiO_2 (P-25) · Photocatalyst · Preferential oxidation of CO (PROX)

1 Introduction

In recent years, fuel cell technology has attracted enormous interest for applications in clean power sources. Especially, polymer electrolyte fuel cell (PEFC) systems are promising candidates for residential and industrial use as well as in automotive applications, although the H_2 must be CO-free to be effectively used as fuel. In this regard, the development of thermal catalytic processes for the preferential oxidation of undesirable CO impurities in H_2 (PROX) has been investigated using noble metal-supported catalysts [1–4].

Meanwhile, various kinds of photocatalysts have also been widely investigated for applications in air and water purification, hazardous waste elimination as well as the production of clean energy resources [5–8]. Among them, TiO_2 has attracted much attention due to its exceptional high reactivity, nontoxicity, chemical stability and low cost. Along these lines, the photocatalytic oxidation of CO with O_2 as well as the photo-assisted water–gas shift reaction have been investigated on TiO_2 and Pt/TiO_2 for the removal of toxic CO [9–11]. Our research has already shown that the photocatalytic preferential oxidation of CO with O_2 in the presence of H_2 (photo-PROX) proceeds efficiently on single-site photocatalysts such as the highly dispersed Mo or Cr oxide species loaded on SiO_2 or MCM-41 [12–14], however, the photo-PROX reaction on TiO_2 loaded with transition metal oxides has yet to be investigated.

In the present study, the photo-PROX reaction was carried out under UV light irradiation at 293 K over transition metal oxide (MoO_3, V_2O_5 and NiO)-loaded and unloaded TiO_2 (P-25) without the use of any precious noble metals. In particular, the effect of the local structure as well as the valence state of the transition metal oxide on CO conversion as well as CO selectivity for the photo-PROX reaction have been examined by various spectroscopic methods.

2 Experimental

Transition metal oxide-loaded TiO_2, i.e., Me/TiO_2, Me = MoO_3, V_2O_5, NiO, were prepared by the impregnation of TiO_2 (P-25 Degussa; pre-calcined at 723 K for

T. Kamegawa · T.-H. Kim · J. Morishima · M. Matsuoka (✉) · M. Anpo (✉)
Department of Applied Chemistry, Graduate School of Engineering, Osaka Prefecture University, 1-1 Gakuen-cho, Naka-ku, Sakai, Osaka 599-8531, Japan
e-mail: matsumac@chem.osakafu-u.ac.jp

M. Anpo
e-mail: anpo@chem.osakafu-u.ac.jp

6 h in air) with an aqueous solution of $(NH_4)_6Mo_7O_{24} \cdot 4H_2O$, NH_4VO_3 and $Ni(NO_3)_3 \cdot 6H_2O$, respectively. After impregnation, the catalysts were calcined at 573 K for 8 h in air. Prior to photocatalytic reactions and spectroscopic measurements, the catalysts were calcined in O_2 (>2.66 kPa) at 723 K for 1 h, and then degassed at 473 K for 1 h. The photocatalytic preferential oxidation of CO with O_2 in the presence of H_2 (photo-PROX) was carried out in a closed system using a quartz reactor under UV light irradiation at 293 K and the reaction products were analyzed by on-line gas chromatography. The yields of CO_2 for the photocatalytic oxidation of CO were corrected by subtracting the amount of CO_2 formed under dark conditions. The catalysts were characterized by various spectroscopic methods such as XRD, UV–Vis, EPR and XAFS measurements. The XAFS spectra of NiO/TiO_2 were recorded at the Ni K-edge absorption in the fluorescence mode at the BL12C facility of the high energy acceleration research organization (KEK) in Tsukuba, Japan. Curve fitting analysis of the EXAFS spectra was conducted on $k^3\chi(k)$ in k-space (k range = 3–12 $Å^{-1}$) with a REX2000 J program (Rigaku).

3 Results and Discussion

Figure 1 shows the CO_2 yields in the photocatalytic preferential oxidation of CO with O_2 in the presence of H_2 (photo-PROX) on TiO_2 and Me/TiO_2 (0.5 wt% as metal oxide, Me = MoO_3, V_2O_5, NiO) under UV light irradiation at 293 K. The CO_2 yield was drastically affected by the kinds of metal oxides loaded on TiO_2. V_2O_5/TiO_2 and MoO_3/TiO_2 exhibited lower photocatalytic activity than that of pure TiO_2, while the reaction rate was remarkably increased by the loading of NiO on TiO_2. The CO_2 yield on NiO/TiO_2 was about 2.5 times higher than that on pure TiO_2, as shown in Fig. 1. It was also found that the CO_2 yields were almost the same in the presence and absence of H_2 in this reaction, suggesting that the CO oxidation reaction was hardly affected by the presence of H_2. After UV irradiation for 3 h, the production of 3.38 μmol CO_2 ($CO_{2\ (t\ =\ 3\ h)}$) and the consumption of 0.06 μmol H_2 ($H_{2\ \mathrm{initial}} - H_{2\ (t\ =\ 3\ h)}$) were observed on NiO/$TiO_2$. CO_2 selectivity was, thus, determined by the following Eq. 1:

$$CO_2\,\mathrm{selectivity}(\%) = \left\{\left(CO_{2(t=3\mathrm{h})}\right)/\left[\left(H_{2\,\mathrm{initial}} - H_{2(t=3\mathrm{h})}\right) + CO_{2(t=3\mathrm{h})}\right]\right\} \times 100. \quad (1)$$

As shown in Table 1, CO conversion as well as CO_2 selectivity on NiO/TiO_2 reached 89 and 98%, respectively, after UV light irradiation for 3 h, showing higher photocatalytic performance than with pure TiO_2 (CO conversion of 81% and CO_2 selectivity of 89% after UV irradiation for 6 h). These results suggest that NiO/TiO_2 can be applied for the photo-PROX reaction at temperatures as low as 293 K. The initial rate of CO oxidation on NiO/TiO_2 (0.5 wt% NiO) was also determined to be 0.63 μmol/min g-cat. This value is lower than those reported for conventional thermal systems which operate at relatively high temperature [2, 3]. However, NiO/TiO_2 photocatalysts provide various advantages toward thermal catalytic systems such as their low operation temperature and the use of non-noble metal elements as their constituents.

The effect of the NiO content on the yields of CO_2 in the photo-PROX reaction has also been investigated. As shown in Fig. 2, the yields of CO_2 increases upon an increase in the NiO loading while passing through a maximum at 0.5 wt% and then decreasing in the region of NiO loadings of higher than 3.0 wt%. These results suggest that the rate of CO oxidation reaction was effectively improved by the loading of small amounts of NiO on TiO_2, especially in the region of NiO loadings of below 0.5 wt%.

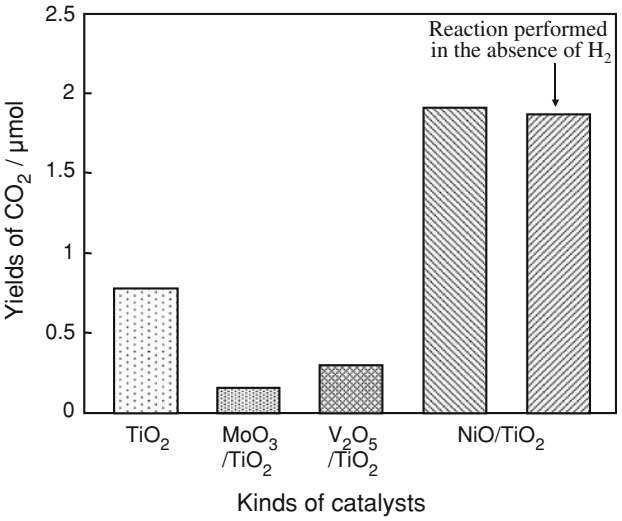

Fig. 1 Yields of CO_2 for the photocatalytic oxidation of CO with O_2 in the presence and absence of H_2 on TiO_2 and Me/TiO_2 (0.5 wt% Me, Me = MoO_3, V_2O_5, NiO) under UV light irradiation at 293 K (Initial amount of gasses: CO = 3.8 μmol, O_2 = 7.5 μmol and H_2 = 24.6 μmol; Amount of catalyst: 50 mg; Reaction time: 60 min)

Table 1 CO conversion and CO_2 selectivity for the preferential photocatalytic oxidation of CO with O_2 in the presence of H_2 on TiO_2 and NiO/TiO_2 (0.5 wt%) under UV light irradiation at 293 K

Catalysts	Reaction time(h)	CO conversion/%	CO_2 selectivity/%
TiO_2 (P-25)	6.0	81	89
NiO/TiO_2 (0.5 wt%)	3.0	89	98

Amount of catalyst: 50 mg

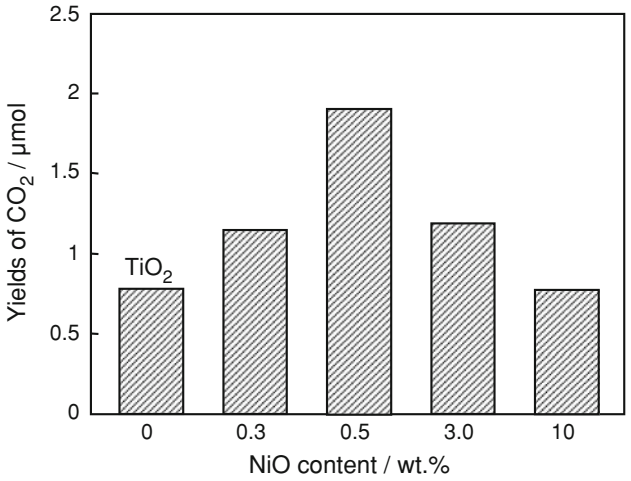

Fig. 2 Effect of NiO loading on the yields of CO_2 for the photocatalytic oxidation of CO with O_2 in the presence of H_2 on NiO/TiO_2 (0, 0.3, 0.5, 3.0, and 10 wt% as NiO) under UV light irradiation at 293 K (Initial amount of gasses: CO = 3.8 μmol, O_2 = 7.5 μmol and H_2 = 4.6 μmol; Amount of catalyst: 50 mg; Reaction time: 60 min)

Characterization studies of NiO/TiO_2 were next carried out by various spectroscopic methods. The absorption edge of the UV–Vis spectra was scarcely seen to change before and after the loading of NiO on TiO_2. Moreover, the XRD patterns of NiO/TiO_2 (0.5 wt%) were almost the same as compared to those of pure TiO_2, indicating that the Ni oxide species were highly dispersed on TiO_2 without the formation of large NiO clusters. The TiO_2 crystallite size of the samples was estimated by applying Scherrer's equation for the (101) reflection of the TiO_2 anatase phase. The TiO_2 crystallite size was determined to be about 20 nm for the series of samples, independent of the kind of the transition metal oxides loaded on TiO_2.

The local structure as well as the valence state of NiO on TiO_2 were also investigated by Ni K-edge XAFS measurements. As shown in Fig. 3, the shapes and the edge positions of the XANES spectra of the NiO/TiO_2 samples (Fig. 3A–C) were very similar to that of bulk NiO as a reference compound (Fig. 3D), showing that the divalent NiO species were supported on TiO_2 without the formation of metallic Ni [15, 16]. Figure 3a–c shows the Fourier transform of EXAFS (FT-EXAFS) of NiO/TiO_2. Two peaks due to the presence of the neighboring oxygen atoms (Ni–O) and nickel atoms (Ni–(O)–Ni) were observed at 1–2 and 2–3 Å, respectively, while the peak corresponding to the Ni–Ni bond of the Ni metal could hardly be seen at around 2 Å (without phase-shift correction) [15, 16]. These results show a good agreement with the XANES results indicating that the divalent NiO species are supported on TiO_2. The relative peak intensity of the neighboring nickel atoms (Ni–(O)–Ni) against the neighboring oxygen atoms

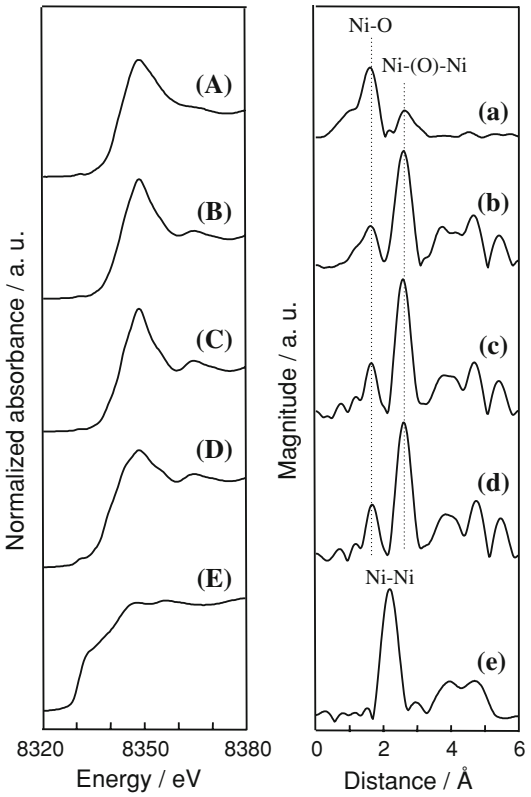

Fig. 3 (*A–E*) Ni K-edge XANES and (*a–e*) Fourier transforms of EXAFS spectra of: (*A, a*) NiO/TiO_2 (0.5 wt%); (*B, b*) NiO/TiO_2 (3 wt%); (*C, c*) NiO/TiO_2 (10 wt%); (*D, d*) NiO; and (*E, e*) Ni foil

(Ni–O) is smaller for NiO/TiO_2 (0.5 wt% NiO) than NiO/TiO_2 (3, 10 wt% NiO) and bulk NiO. Furthermore, as shown in Table 2, curve-fitting analysis of FT-EXAFS revealed that the coordination number (CN) of both the Ni–O and Ni–(O)–Ni shells of NiO/TiO_2 increased with an increase in the NiO content [16]. These results clearly suggest that the particle size of the NiO species is significantly reduced for NiO/TiO_2 with low NiO loadings of

Table 2 Curve fitting results of the Ni K-edge EXAFS spectra of NiO and NiO/TiO_2 (0.5, 3, 10 wt% NiO)

Samples	Shell	R[a]/Å	CN[b]
Ni foil	Ni–Ni	2.47	12
NiO	Ni–O	2.07	6.0
	Ni–(O)–Ni	2.94	12
NiO/TiO_2 (0.5 wt%)	Ni–O	2.04	4.07
	Ni–(O)–Ni	3.02	4.83
NiO/TiO_2 (3 wt%)	Ni–O	2.07	5.87
	Ni–(O)–Ni	2.96	11.1
NiO/TiO_2 (10 wt%)	Ni–O	2.07	5.91
	Ni–(O)–Ni	2.95	11.4

[a] Bond distance

[b] Coordination number

below 0.5 wt% and these highly dispersed NiO clusters play an important role as additives for the photo-PROX reaction.

In order to elucidate the role of the small NiO clusters as additives to enhance the photo-PROX reaction rate, the charge separation characteristics of NiO loaded and unloaded TiO_2 were investigated by EPR measurements. It is known that the Ti^{3+} species are formed on TiO_2 by trapping the photogenerated electrons under UV light irradiation in vacuum [17, 18]. Up to now, the effect of the Pt particles supported on TiO_2 on the formation of the Ti^{3+} species have been investigated in detail [19, 20]. It has been demonstrated that the photogenerated electrons were efficiently transferred from TiO_2 to the Pt particles over the Pt/TiO_2 systems, preventing the formation of the Ti^{3+} species and electron-hole recombination [19, 20]. Figure 4 shows the EPR spectra of the pure TiO_2 and NiO/TiO_2 before (dotted line) and after UV light irradiation (solid line) under vacuum at 77 K for 1 h. Under UV irradiation at 77 K, the intensity of the signal, which can be assigned to the Ti^{3+} species in anatase ($g_\perp = 1.991$, $g_\parallel = 1.961$) and rutile ($g_\perp = 1.980$) [17, 18], increased with the irradiation time. However, in the case of NiO/TiO_2, the change in the EPR signal due to the Ti^{3+} species was small as compared to those of pure TiO_2 after UV light irradiation. The increased efficiency of CO oxidation on NiO/TiO_2 can, thus, be ascribed to the suppression of the electron-hole recombination which was realized through electron trapping by NiO, i.e., the transfer of the photoformed electrons from TiO_2 to NiO [16, 21]. On the other hand, femtosecond pump-probe diffuse reflectance investigations have revealed that the recombination rate of the photogenerated electrons and holes on TiO_2 is decreased by the loading of MoO_3, V_2O_5 and CrO_3 [22]. In fact, the photocatalytic activity of TiO_2 for the oxidation of 4-nitrophenol was decreased by the loading of MoO_3 and V_2O_5 on TiO_2 [22]. Therefore, it could be considered that the same phenomena occurred in the present reaction systems, leading to the decreases in the CO oxidation rate on MoO_3/TiO_2 and V_2O_5/TiO_2 as compared to pure TiO_2.

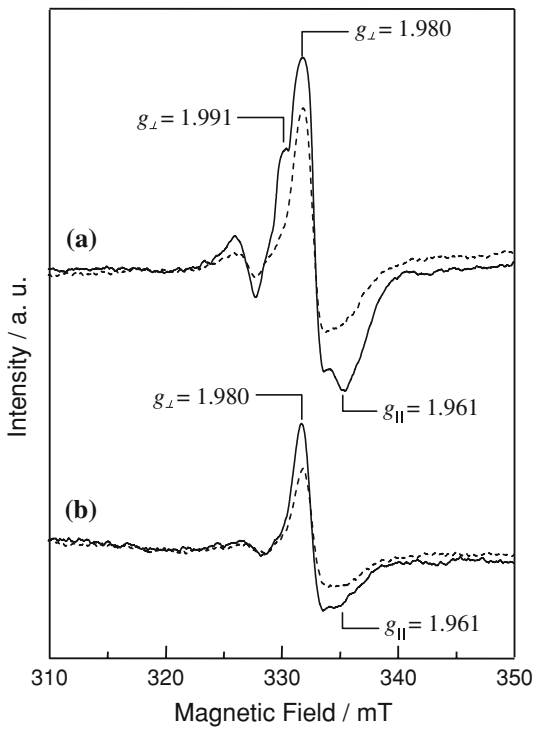

Fig. 4 (*a*) EPR spectra of TiO_2 and (*b*) NiO/TiO_2 (0.5 wt%) measured at 77 K before (*dotted line*) and after UV light irradiation (*solid line*) in vacuum at 77 K for 1 h

The selectivity for the oxidation of CO with O_2 in the presence of H_2 was also improved by the loading of NiO on TiO_2 (Table 1). According to these characterization studies, highly dispersed NiO particles were formed on TiO_2 at low NiO content, leading to the formation of large numbers of coordinatively unsaturated NiO sites. The thus-formed unsaturated NiO sites act as efficient adsorption sites for gaseous CO and increases the surface concentration of CO on NiO/TiO_2 compared with H_2. In fact, a CO-adsorbed species has been observed on various coordinatively unsaturated Ni cations (Ni^{2+} and Ni^{+}) of NiO at room temperature by FT–IR investigations [23, 24]. Therefore, the large difference in the surface concentration of CO and H_2 can be the reason that the CO oxidation rate was hardly affected by the presence of H_2, as shown in Fig. 1. Moreover, the high reaction rate and CO_2 selectivity of NiO/TiO_2 can be ascribed to the higher surface concentration of CO on NiO/TiO_2 than the unloaded TiO_2 since CO oxidation on TiO_2 proceeds through the reaction between the photoformed active oxygen species (O^-, O_2^-, O_3^-) and the CO-adsorbed species formed on the surface of TiO_2 [9]. A more detailed study of the mechanisms behind the photo-PROX reaction on NiO/TiO_2 is now underway.

4 Conclusions

It was found that the photocatalytic preferential oxidation of CO with O_2 in the presence of H_2 (photo-PROX) proceeded efficiently on NiO/TiO_2 (0.5 wt% NiO) with a high CO_2 selectivity under UV light irradiation at 293 K, exhibiting around 2.5 times higher photocatalytic activity than pure TiO_2. XAFS investigations revealed that the highly dispersed NiO species on TiO_2 at low NiO loadings of 0.5 wt% acted as efficient additives to improve the photo-PROX reaction rate. Moreover, EPR investigations suggested that the highly dispersed NiO species plays an important role in realizing the efficient charge separation of

the photoformed electrons and holes through electron transfers from TiO_2 to NiO, leading to the high photocatalytic performance of NiO/TiO_2.

Acknowledgments This work was supported by the Kansai Research Foundation (KRF) for Technology Promotion and we would like to express our appreciation for their kind support.

References

1. Echigo M, Shinke N, Takami S, Higashiguchi S, Hirai K, Tabata T (2003) Catal Today 84:209
2. Kuriyama M, Tanaka H, Ito S, Kubota T, Miyao T, Naito S, Tomishige K, Kunimori K (2007) J Catal 252:39
3. Manasilp A, Gulari E (2002) Appl Catal B Environ 37:17
4. Landon P, Ferguson J, Solsona BE, Garcia T, Carley AF, Herzing AA, Kiely CJ, Golunski SE, Hutchings GJ (2005) Chem Commun 3385
5. Anpo M (2004) Bull Chem Soc Jpn 77:1427
6. Fujishima A, Rao TN, Tryk DA (2000) J Photochem Photobiol C Photochem Rev 1:1
7. Matsuoka M, Kitano M, Takeuchi M, Tsujimaru K, Anpo M, Thomas JM (2007) Catal Today 122:51
8. Kudo A (2003) Catal Surv Asia 7:31
9. Sato S, Kadowaki T (1987) J Catal 106:295
10. Hwang S, Lee MC, Choi W (2003) Appl Catal B Environ 46:49
11. Sato S, White JM (1980) J Am Chem Soc 102:7206
12. Kamegawa T, Takeuchi R, Matsuoka M, Anpo M (2006) Catal Today 111:248
13. Matsuoka M, Kamegawa T, Anpo M (2007) Stud Surf Sci Catal 165:725
14. Kamegawa T, Morishima J, Matsuoka M, Thomas JM, Anpo M (2007) J Phys Chem C 111:1076
15. Domen K, Kudo A, Onishi T, Kosugi N, Kuroda H (1986) J Phys Chem 90:292
16. Kato H, Asakura K, Kudo A (2003) J Am Chem Soc 125:3082
17. Hurum DC, Agrios AG, Gray KA, Rajh T, Thurnauer MC (2003) J Phys Chem B 107:4545
18. Nakaoka Y, Nosaka Y (1997) J Photochem Photobiol A Chem 110:299
19. Ward MD, Bard AJ (1982) J Phys Chem 86:3599
20. Anpo M, Aikawa N, Kubokawa Y (1984) J Phys Chem 88:3998
21. Kudo A, Domen K, Maruya K, Onishi T (1987) Chem Phys Lett 133:517
22. Paola AD, Marcì G, Palmisano L, Schiavello M, Uosaki K, Ikeda S, Ohtani B (2002) J Phys Chem B 106:637
23. Escalona Platero E, Coluccia S, Zecchina A (1985) Langmuir 1:407
24. Parizotto NV, Rocha KO, Damyanova S, Passos FB, Zanchet D, Marquws CNP, Bueno JMC (2007) Appl Catal A Gen 330:12